JOURNAL OF
ENVIRONMENTAL HYDROLOGY
The Electronic Journal of the International Association for Environmental Hydrology
On the World Wide Web at http://www.hydroweb.com
VOLUME 16 2008

IMPROVED DEPTH OF PENETRATION OF GEOELECTRIC IMAGING IN A CONFINED AREA USING REFRACTION TOMOGRAPHY

I.B. Osazuwa[1]
C.C. Chiemeke[1]
N.K. Abdullahi[1]
C.C. Akaolisa[2]

[1]Advanced Geophysical Research Laboratories
Ahmadu Bello University, Zaria, Nigeria
[2]Department of Geology, Federal University of Technology
Owerri, Nigeria

Geo-electric and seismic refraction tomography were carried out to investigate the depth to basement complex in a confined area where there are serious limitations in spread length as a result of obstacles. The major instruments used for this survey where Terraloc Mark6 digital seismograph, sets of vertical geophones, SAS 4000 Terrameter and Electrode Selector ES 464. The layout geometry was such that both the receivers and source were in a straight line. The 24 geophones and the source point were located at intervals of 5 m, for a spread length of 120 m. In addition to the initial shot point, shots were fired at each geophone point. In the case of the geo-electric survey, the electrodes were laid out along the profiles at an interval of 2.5 m between the 41 electrodes, for a spread length of 100 m. In each of the profiles, geo-electric tomography was only able to penetrate down to a depth of 15 m at optimum current ejection into the subsurface. The geo-electric tomography could not reach the basement rock, except for the points where the basement complex is at a depth shallower than or equal to 15 m. For seismic refraction tomography the depth of penetration was greater than 30 m. It was possible to delineate the basement topography beyond a depth of 15 m along the profiles.

INTRODUCTION

The purpose of electrical surveys is to determine the subsurface resistivity distribution by making measurements on the ground surface. From these measurements, the true resistivity of the subsurface can be estimated. The ground resistivity is related to various geological parameters such as the mineral and fluid content, porosity, and degree of water saturation in the rock. Electrical resistivity surveys have been used for many decades in hydrogeological, mining and geotechnical investigations. More recently, it has been used for environmental surveys (Loke, 2000).

The refraction method is mainly used for mapping of the weathered layer, for determining depth to water table, for engineering purposes, and for applying correction to reflection data (Osemeikhian et al., 1994).

When the refractor is suspected to have a dip, the velocities of the beds and the dip of the interface can be obtained by shooting a second complementary profile in the opposite direction. (Lowrie, 1997).

Near-surface seismic refraction tomography is a geophysical inversion technique designed for subsurface investigations where seismic propagation velocity increases with depth. The output of refraction tomography analysis is a model of the distribution of seismic velocities in the subsurface; thus, additional interpretation must occur to generate a geologic model (i.e., determination of what the velocities represent) (Gregory, 2002).

Both methods were applied in an area where there are serious limitation in spread length as a result of the presence of buildings and very busy road network surrounding the area. The spread length determines the depth of penetration of both the geo-electric and the seismic methods. In a situation where both methods have approximate equal spread length, experiment has shown that the seismic refraction method penetrates to a greater depth than the geo-electric method.

The aim of the present work includes to determine the maximum depth of penetration of seismic refraction tomography in comparison to geo-electric tomography of nearly equal spread length taken simultaneously along the same profile, and to delineate the basement topography.

The instruments employed for this work include the Terraloc Mark 6 24 channel digital seismography, with a very high dynamic range for both reflection and refraction survey, and sets of vertical geophones, with a frequency range of 4 to 100 Hz. Other instrument include, reels of cable, a sledge hammer for energy source, SAS 4000 Terrameter, Electrode Selector ES 464 and 41 sets of steel electrodes.

Location and Geology of Study Area

The study area, Figure 1, Lokoja New General Hospital in Kogi State, North Central Nigeria is located at Latitude 8^0 N and Longitude 6^0 E. The Precambrian basement complex rocks in the area are overlain by crystalline generally folded rocks. The ancient crystalline rocks are composed of gneisses, migmatite, quartzite, schist and granites. In general, the laterite is underlain by basal conglomerate with clay and alluvial gravel materials and hard fissured rocks (Mcurry, 1976).

METHODOLOGY

The field procedure employed for the geo-electric imaging, included laying out the 42 steel electrodes along the profile which was connected to the multicore cable at 5 m regular take-out intervals via sets of jumpers. This was adapted for the purposes of 2.5 m electrode spacing in most

of the profile. The measurement of the apparent resistivity of the subsurface was carried out by the electrode selector ES 464 and the SAS 4000 Terrameter, where it was stored for onward processing.

The seismic refraction method was conducted by planting the geophones at regular intervals of 5 m along the profile. An initial offset distance of 15 m was used, shots were fired at a regular interval distance of 2.5 m before the first geophone at each geophone point, in between the geophones and beyond. The generated seismic refracted wave and its resultant seismogram were recorded by the seismograph where it was stored for further processing.

DATA PROCESSING

The processing of the measured geo-electric data was done using 2-dimensional resistivity imaging interpretation software. This interpretation software essentially calculates the true resistivity and true depth of the ground from the input data (apparent resistivity) file using a Jacobian matrix calculation with forward modeling procedures and robust least squares inversion algorithm with smoothing constraints. The results of the interpretation are displayed as a 2-D electrical resistivity image of the subsurface along the line of the traverse. Calculated pseudosections were produced as replicas of the observed, and the corresponding true resistivity model was generated.

Spectrum analysis was carried out on the raw seismic data to determine the dominant frequency which constitutes the important seismic signal. A bandpass frequency was set to eliminate the seismic noise which could have marred the real seismic signals. The gain filter was applied to enhance the amplitude of the far trace. The first arrival times was then picked and used for inversion to generate a tomographic model, using the waveform inversion method.

The various theories of the two methods are outlined below.

The resistivity measurements are normally made by injecting current into the ground through two current electrodes (C1 and C2 in Figure 2), and measuring the resulting voltage difference at two potential electrodes (P1 and P2). From the current (I) and voltage ($\mathbf{V}$) values, an apparent resistivity (ρ_a) value is calculated.

$$\rho_a = \frac{kV}{I} \tag{1}$$

where k is the geometric factor which depends on the arrangement of the four electrodes.

Resistivity meters normally give a resistance value, $R = V/I$, so in practice the apparent resistivity value is calculated by

$$\rho_a = kR \tag{2}$$

The calculated resistivity value is not the true resistivity of the subsurface, but an “apparent” value which is the resistivity of a homogeneous ground which will give the same resistance value for the same electrode arrangement. The relationship between the “apparent” resistivity and the “true” resistivity is a complex relationship. To determine the true subsurface resistivity, an inversion of the measured apparent resistivity values using a computer program must be carried out (Loke, 2000).

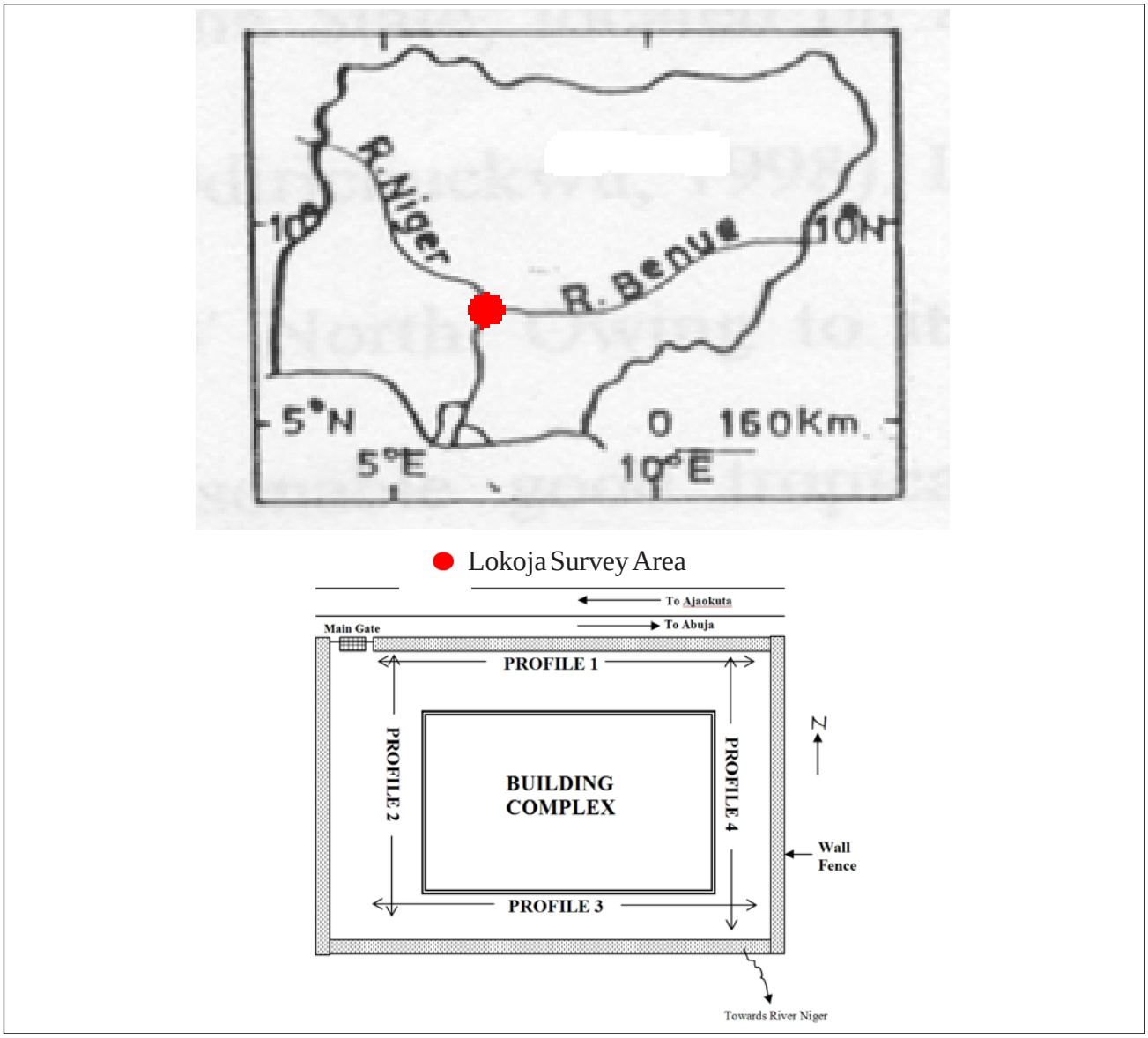

Figure 1. Sketch of the survey area not drawn to scale.

The series expansion method which includes curved ray paths was used in the model computation of the seismic refraction tomography model. Thus for a given source receiver pair the line integral of the model function *M(r)* over the raypath is

$$p_{obs} = \int_{ray} M^{true}(r)dr \tag{3}$$

where the observed projection given by the data function p_{obs} represents the measured line integral (observed tomography data) and $M^{true}(r)$ is the true model function which remains to be determined. The last equation is used to formulate the forward modeling by setting

$$p = \int_{ray} M(r)dr \tag{4}$$

where p is now the predicted function and $M(r)$ is the estimated model function. Thus forward modeling is defined as determining the predicted data function from the line integral along the raypath through known, but estimated, model function.

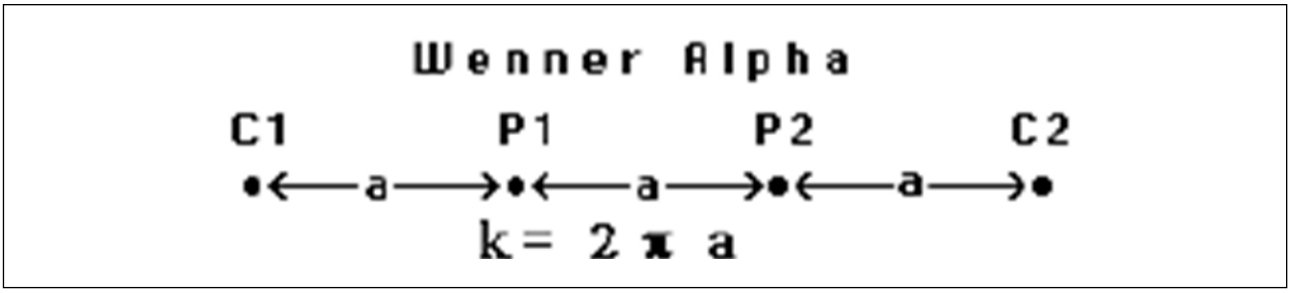

Figure 2. Wenner array with its geometric factors k.

For a discretized model function Equation 4 is rewritten in discrete form, to describe ray through the discrete model function as

$$p = \sum_{j=1}^{j} M_j S_j \tag{5}$$

where M_j is the estimated model function for the jth cell, S_j is the raypath length of the ray within the jth cell, and J is the total number of cells in the gridded target.

The addition of extra rays will make all the cells to be interrogated by this network of rays. Therefore we modify the index of Equation (4) to include a projection value for every ray. If p_i represents the projection, or line integral predicted for the i^{th} ray, then Equation (4) is rewritten as

$$p = \sum_{j=1}^{j} M_j S_{ij} \quad \text{for } i=1...I \tag{6}$$

where I is the total number of rays, S_{ij} is the path length of the i^{th} ray through the j^{th} cell (Tien-When, 2002).

RESULTS AND DISCUSSION

The inverse models for electrical resistivity and seismic tomography data along Profile 1 are shown in Figure 3. The electrical resistivity model has a spread length of 100 m and 1820 data points. The measured apparent resistivity data correlate very well with the calculated apparent resistivity data as can be seen in the two pseudosections presented in Figure 3, therefore the model of the true resistivity can be accepted.

However a comparison of their depth section indicated that the geo-electric section probed down to a depth of 14.6 m, while the seismic section indicated a depth of penetration of beyond 30 m.

The velocity values of the seismic tomography above 3000 m/s indicated that it probed up to the basement, unlike the resistivity section which indicated very low resistivity for two reasons. First, because the area is waterlogged, it tends to have a very high conductivity, and secondly, because the resistivity model did not get to the basement as a result of spread length limitation.

The inverse models for electrical resistivity and seismic tomography for Profile 2 are shown in Figure 4.

The model section of the electrical resistivity method indicated that the current only penetrated to a depth of 11 m, thereby giving rise to low resistivity values which is slightly higher than the

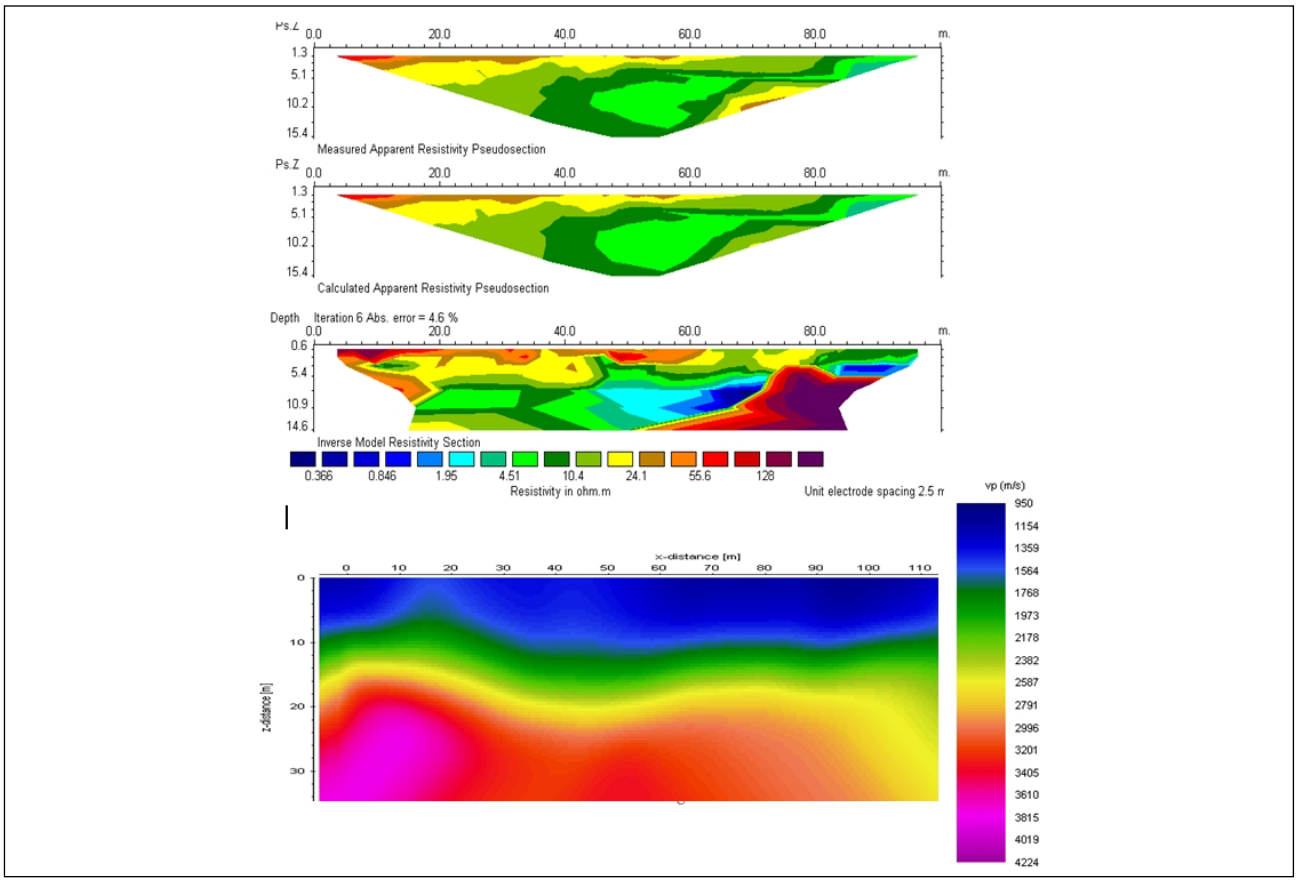

Figure 3. Geo-electric and seismic tomography models for Profile 1.

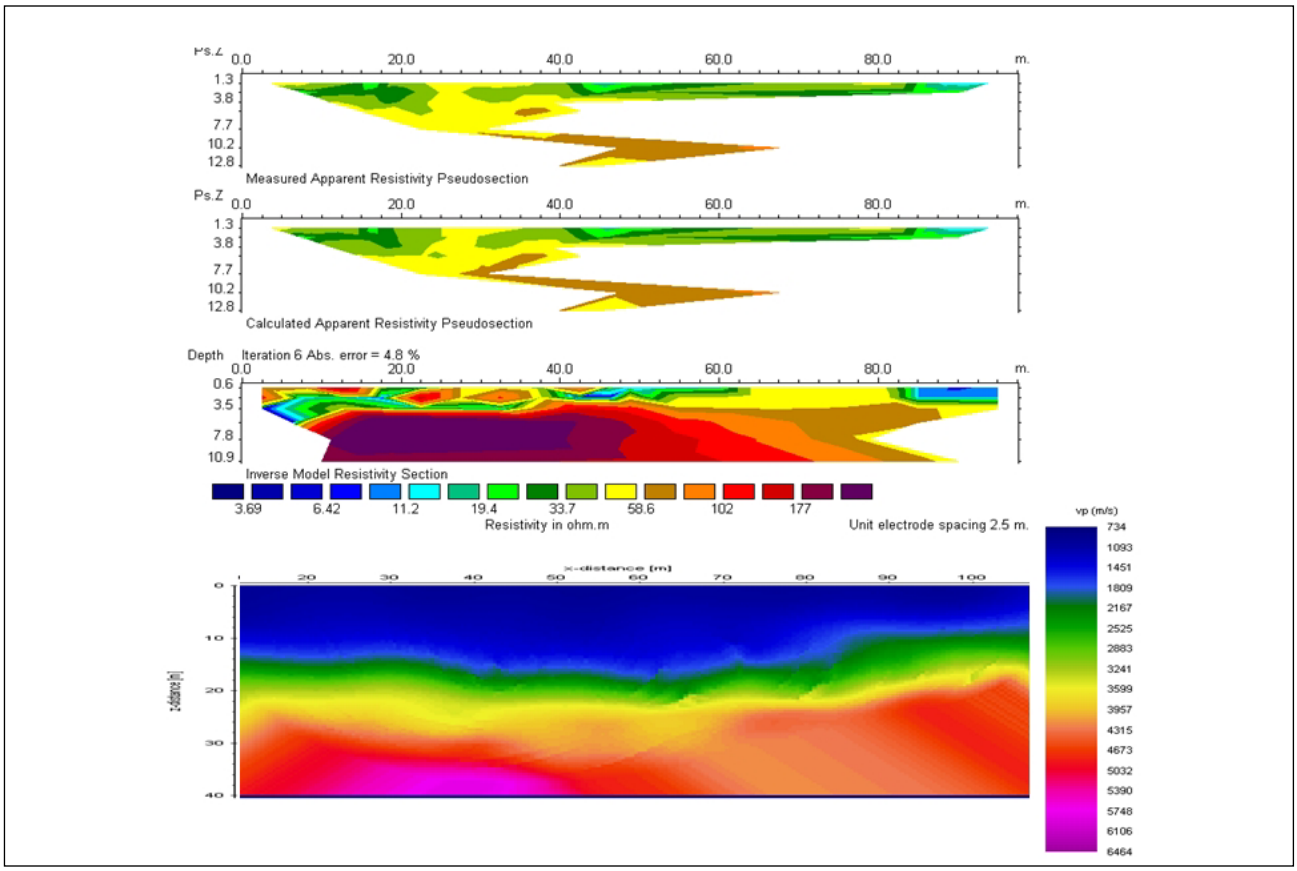

Figure 4. Geo-electric and seismic tomography models for Profile 2.

values of Profile 1. This is not unconnected to the limitation in spread length, which prevented the ejected optimum current from getting to the basement.

However, seismic tomography of the same spread length and taken along the same profile, was able to probe up to a depth of 40 m, with very high resolution. The range of velocity indicated in the velocity color bar for the model, is a clear indication that the seismic energy probed to the basement.

The inverse model for electrical resistivity and seismic tomography for Profile 3 are shown in Figure 5. The electrical resistivity model for the profile which was taken in the same survey area serves as a good control for the other profiles, because it has no limitation of spread length. It has a spread length of 200 m at a 5 m interval between electrodes, hence it was possible for the optimum current ejected into the ground to penetrate to a depth of 30 m. The resistivity values indicated on the model, which are on the high side, also indicated that the current was able to probe to the basement. The corresponding seismic tomography model as usual was able to probe beyond 30 m, and showed an indication of high velocity which is the characteristic of a basement rocks.

Geologic Outlines of the Seismic Profiles

Figure 6 depicts the geologic outlines of the weathered and fresh basement topography of the seismic profiles. The limit of the overburden outlined in Profile 1 showed that the basement has been weathered down to a depth of about 13 m. The thickest part of the overburden corresponds to a water bearing formation identified based on the velocity and visible seepage at the surface. The thickness of weathered basement along the profile varies from 4 m to 7 m.

Profile 2 showed that the weathered basement has been weathered to a depth of 18 m which

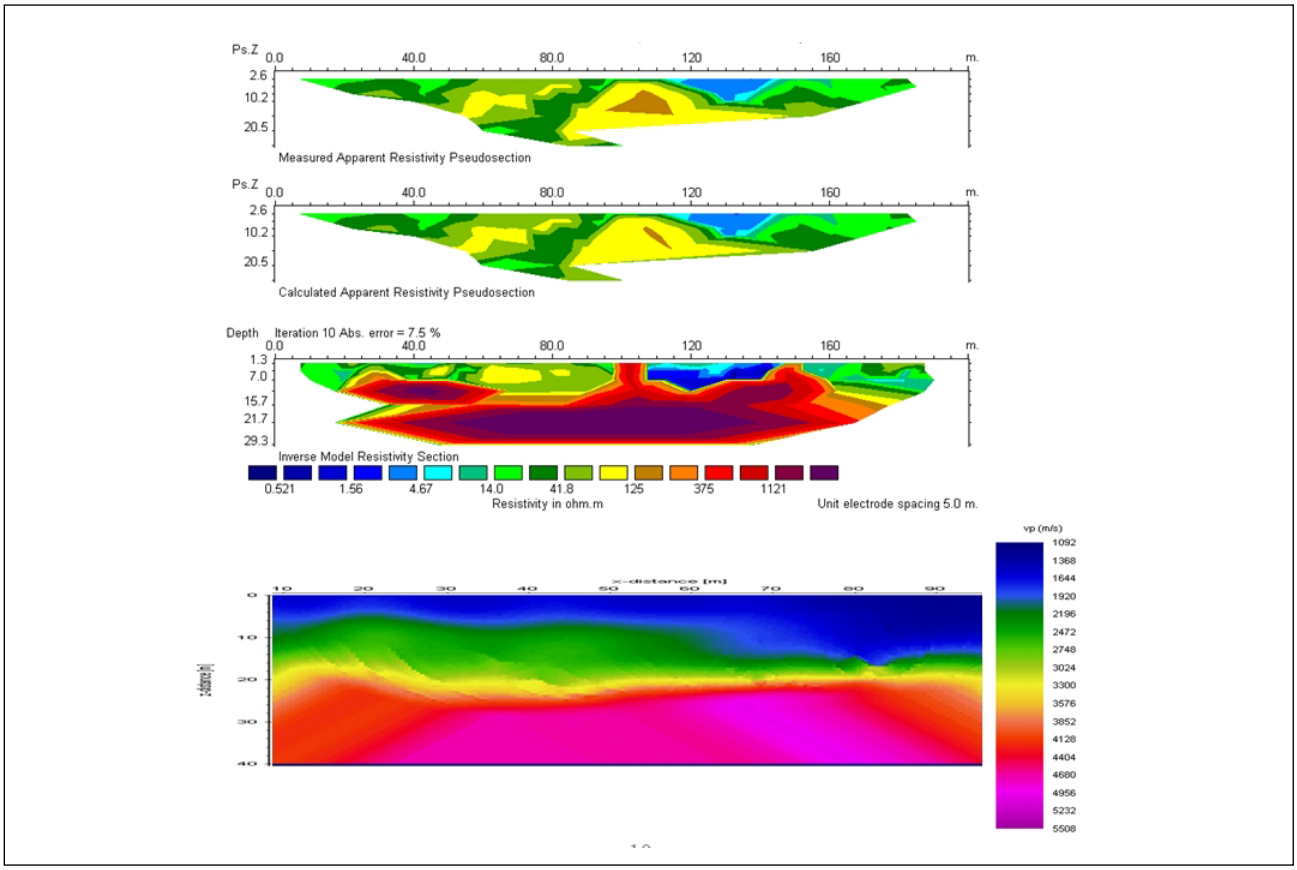

Figure 5. Geo-electric and seismic tomography models for Profile 3.

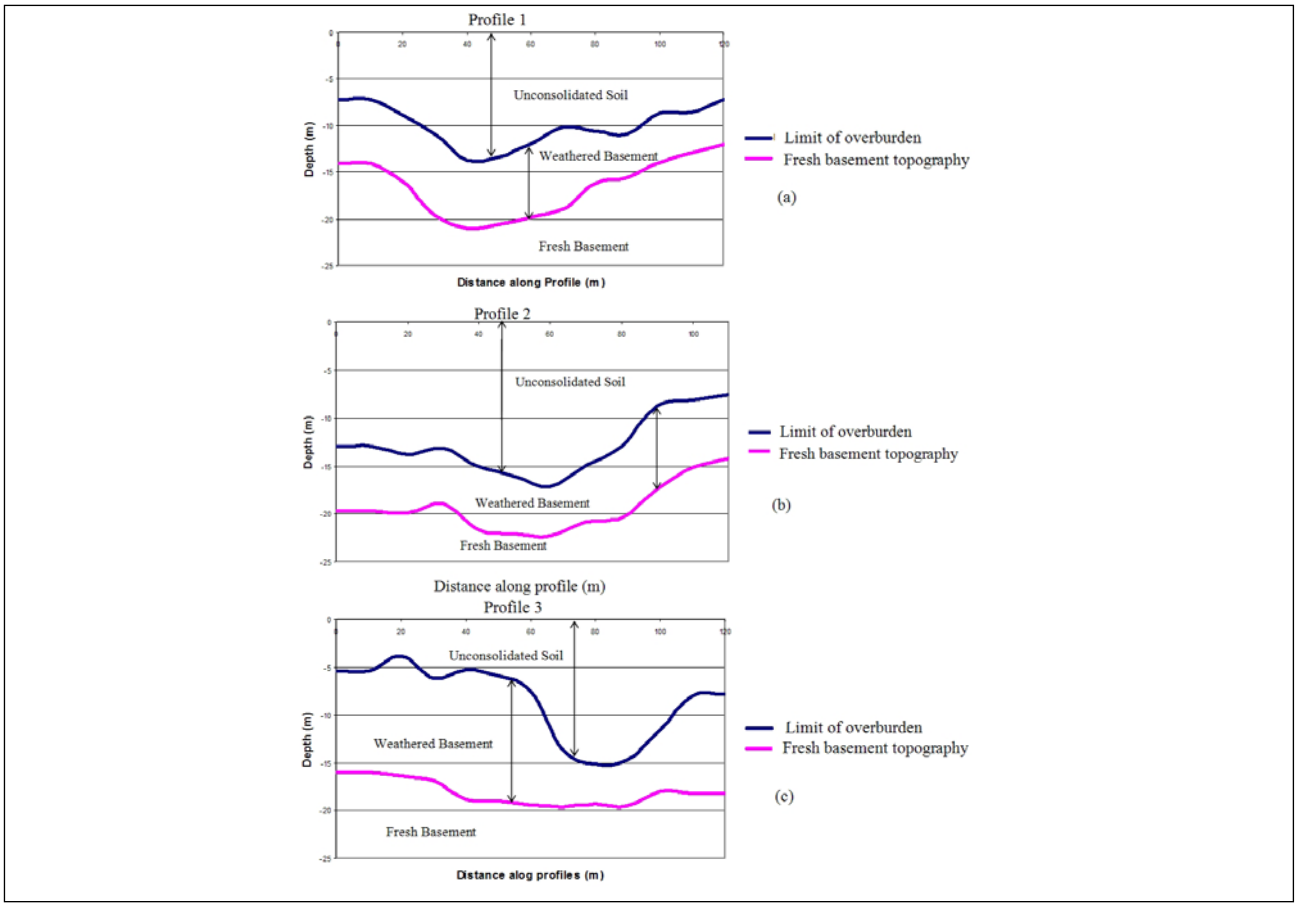

Figure 6. Overburden and weathered basement thickness overlying the fresh basement along (a) profile 1 (b) profile 2 and (c) profile 3 deduced from seismic data.

marks the thickest part of the overburden. The thickness of the weathered basement along the profile varies from 4 m to 6 m. The weathered basement and the fresh basement topography had corresponding undulations.

Profile 3 showed relatively thin overburden thicknesses at the beginning of the profile, which was followed by what appeared to be a buried valley towards the end of the profile. This also corresponds to a water bearing formation which was identified as a result of the seepage to the surface and the recorded seismic velocity. Unlike the overburden, the weathered basement is thicker at the beginning of the profile than toward the end of the profile. The fresh basement maintained a relatively flat topography along the profile. The mapping was possible as a result of the high depth of penetration by seismic refraction tomography. The overburden and weathered basement thicknesses could not be mapped along the resistivity profile because of the low depth of penetration, since it only probed the shallow part of the formation that is highly heterogeneous. However, the fresh basement topography marks the locus of points at the local lower limit of the weathered basement at depth along each of the profiles. The values for the different formation thickness and depths are shown in Table 1.

CONCLUSION AND RECOMMENDATION

It is obvious that seismic refraction tomography probes deeper than geo-electric tomography at the same spread length. The geo-electric section indicated very low velocity, which is a clear indication that it did not probe down to the basement. Seismic refraction tomography on the other

Table 1. Statistics of the overburden and weathered basement under the three profiles.

Formation	**Range of thickness (m)**			**Range of Depth of Lower Limit below ground surface (m)**		
	Profile 1	Profile 2	Profile 3	Profile 1	Profile 2	Profile 3
Overburden	7 to 13	8 to 17	3 to 16	7 to 13	8 to 17	3 to 16
Weathered basement	4 to 7	4 to 6	4 to 14	12 to 21	14 to 23	14 to 19

hand gave several indications of high velocities in the area which showed that it was able to probe down to the basement. Seismic refraction tomography was able to delineate the basement topography beyond a depth of 15 m.

It is recommended that seismic refraction tomography be employed in an area where there are serious limitations in spread length to probe a particular depth of interest by increasing the energy source.

ACKNOWLEDGMENT

The authors are grateful to Professor J.E.A. Osemeikhian of the Physics Department, Ambrose Alli University, Ekpoma, Edo State, Nigeria and Dr H.O. Aboh, Physics Department, Kaduna State University for reviewing the paper which greatly improved the quality of the research work. The International Programme in the Physical Sciences (IPPS), Uppsala University, Sweden is acknowledged for providing the equipment and computational facilities used for this research work

REFERENCES

Gregory, S.B. 2002. Near-Surface Seismic Refraction Tomography Tutorial.

Loke, M.H. 2000. Electrical imaging surveys for environmental and engineering studies, a practical guide to 2-D and 3-D surveys.

Lowrie, W. 1997. Fundamental of Geophysics, Cambridge University Press

McCurry, P .1976. The geology of the Precambrian to lower Paleozoic rocks of Northern Nigeria - A review in Kogbe, C.A.(Editor). Geology of Nigeria. Elizabeth Publication Company, Lagos. Nigeria. P 15-40

Osemeikhian, J.E.A., and M.B. Asokhia. 1994. Applied Geophysics, Stamatas Services Ltd.

Tien-When, L., and L. Philips. 2002. Fundamentals of Seismic Tomography. Society of Exploration Geophysicists.

ADDRESS FOR CORRESPONDENCE
Nasir Khalid Abdullahi
Advanced Geophysical Research Laboratories
Department of Physics
Ahmadu Bello University
Zaria, Nigeria

Email: nasirasman@yahoo.com